University of Baghdad
College of Engineering
JOURNAL OF ENGINEERING

Journal of Engineering
journal homepage: www.jcoeng.edu.iq
Volume 32 Number 2 February 2026

Contribution of Fill-Concrete Compressive Strength on the Structural Performance of CFSST Columns: An Analytical Study

Shatha D. Mohammed *, Mohammed Riyadh Khalaf, Teghreed H. Ibrahim, Abbas A. Allawi

Department of Civil Engineering, College of Engineering, University of Baghdad, Baghdad, Iraq

ABSTRACT

High-rise structures are a significant indication in contemporary urban improvement, mainly in areas characterized by accelerated urban growth and dense population. This type of building should be designed to withstand severe load conditions. Therefore, using composite structural elements in such structures is required for stronger and durable elements. This paper introduces a finite element analysis model for Concrete Filled Stainless Steel Tubular Columns (CFSST) of (100x100) mm cross-section and (1250) mm length to inspect the impact of concrete compressive strength on the response of (CFSST). The generated model was first evaluated through a comprehensive comparison with experimental research. Then, after the model was used to study the considered parameter, namely, concrete compressive strength. A wide range of concrete compressive strengths was included (45, 50, 55, 60, 65, 70, and 75) MPa. FE results indicated that the CFSST columns' ultimate strength is directly proportional to the fill-concrete compressive strength. The optimum gained load capacity was (416 kN) when the concrete strength was 75MPa. The modification of increasing fill-concrete compressive strength extended to include the stiffness, toughness, and the yield load to be (89, 38.9, and 64%), respectively, as the strength increased to 75MPa. The response improvement didn't include the ductility index. A reduction in the ductility index was observed as the filled-concrete compressive strength increased, reaching 15.4% when the compressive strength reached 65 MPa. This reduction remains constant, even though the compressive strength increases (from 70 to 75 MPa).

Keywords: CFSST column, Concrete compressive strength, Ductility index, Absorbed energy, Stiffness.

1. INTRODUCTION

The demand for high-rise structures and the requirement for more flexible structural systems capable of resisting severe lateral stresses caused by wind and earthquake events demand the use of mixed steel and concrete systems. This results in the development of

*Corresponding author
Peer review under the responsibility of University of Baghdad.
https://doi.org/10.31026/j.eng.2026.02.08

Article received: 26/09/2025
Article revised: 16/10/2025
Article accepted: 24/12/2025
Article published: 01/02/2026

Concrete Filled Steel Tubular Columns (CFST) members. Generally, the Concrete Filled Stainless Steel Tubes (CFSST) member has almost all the identical advantages as the CFST members. Still, the CFSST members achieve higher corrosion resistance and better final finishing than ordinary carbon steel. In recent years, the behavior of CFST columns has been studied by several researchers **(Rasmussen, 2020).** An expanded investigation for the structural behavior of steel tuber columns filled with concrete was performed by **(Alrebeh and Ekmekyapar, 2019; Lam and Williams, 2004; Zeghiche and Chaoui, 2005).** The uniaxial strength of the CFST columns was experimentally evaluated throughout different internal construction characteristics **(Dong et al., 2018; Dai and Lam, 2010).** Moreover, the influence of the CFST column slenderness ratio was studied considering different parameters **(Uy, 2000; Mursi and Uy, 2004; Uy et al., 2011).** The interaction diagram of the CFST column was deeply investigated by several studies, including the effect of fill-concrete compressive strength and strengthening process **(Al-Sherrawi et al., 2025; Salman and Al-Sherrawi, 2024)**. The reviews indicate that the bearing capacity of almost CFST members studied in the literature was enhanced by using the fill-concrete in the tube, and also, the local steel tube buckling was reduced. **(Tokgoz et al., 2021)** studied that are eccentrically loaded under biaxial bending and axial compression. The tested specimens were divided into two groups (I and II), each with a different embedded steel section, as shown in **Fig. 1**. Both groups included five columns; three specimens were filled with plain concrete and tested under different eccentricities (55, 65, and 70) mm, respectively. The other two were of steel fiber-reinforced concrete and tested under eccentricities of (55 and 65) mm, respectively. A theoretical model that considered the role of structural steel elements was used to predict the strength and load-deflection behavior of CFSST composite columns. It was found that the behavior of the CFSST column was in a ductile manner. Three materials (carbon steel, concrete, and stainless steel tube) have a significant effect on the ultimate load. The buckling due to the existence of the infill concrete and the presence of steel fiber influences the structural behavior.

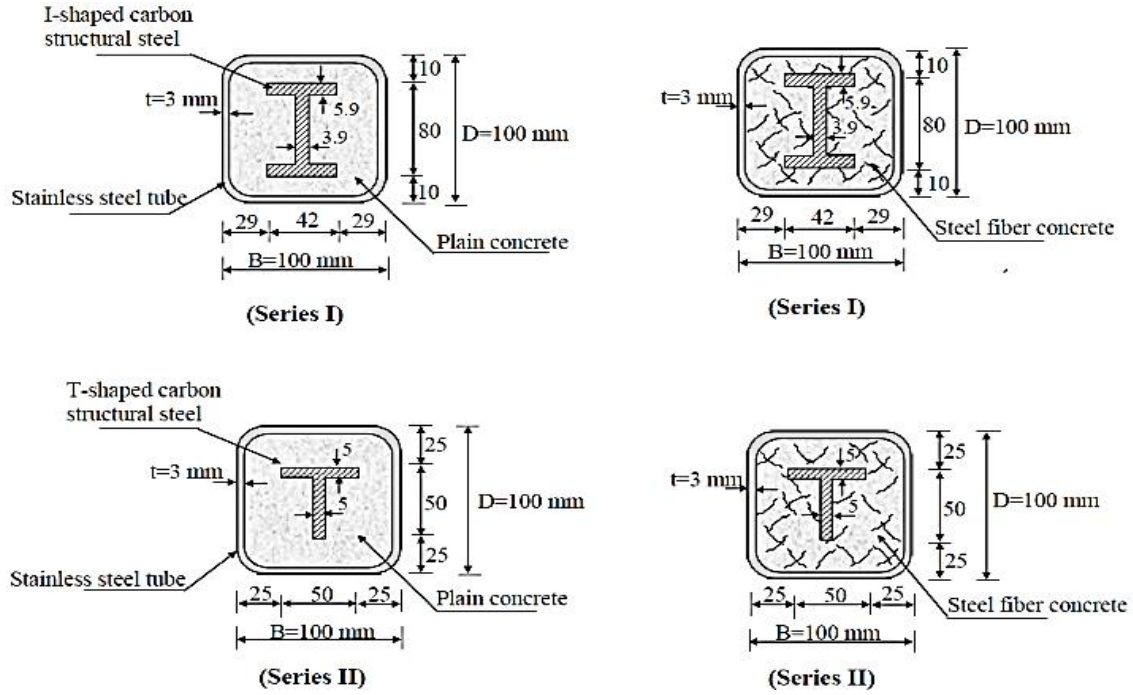

Figure 1. Specification of the tested columns **(Tokgoz et al., 2021).**

(Manikanta et al., 2020). inspected, experimentally and theoretically, the structural performance of a CFSST stub column with a circular cross-section under axial loading. It was observed that increasing the aspect ratio caused an increase in the capacity of the CFSST column carrying load. The failure mode of the specimens was inward buckling (due to the existence of the infill concrete). The cracks were formed in the face of the CFSST column, and Stainless steel can hold more weight than other materials; for that, it was better to use the CFSST column in high-performance buildings and harsh environments. **(Hassanein et al., 2020)** presented an inelastic analysis for circular CFSST columns subjected to axial loading that proved the necessity for changing the Eurocode design model for thin column infill with concrete in the next versions by considering the accurate buckling curve. **(Kazemzadeh Azad et al., 2021)** investigated the performance of compact and slender boxes of CFSST tubular members under axial loading. Four groups were considered (A, B, C, and D) to represent a short column under compressive loading, a beam under bending loading, a short column under both axial and bending loading, and a long column under axial loading, respectively. Then, a numerical analysis was conducted using ABAQUS software. Based on the results, criteria for categorizing CFSST were developed. Closure design formulas for compact and slender CFSST structures subjected to axial compression or pure bending were then established using experimental and numerical results. Local buckling was considered in the developed processes.

The behavior of concrete-filled steel tube CFST columns under axial compression load was reviewed. So many parameters affect the bearing capacity of CFST columns, such as the width-to-thickness ratio, concrete compressive strength **(Liu, 2004; Liu, 2005; Liu, 2006; Lee et al., 2011)**, the mechanical properties of the steel tube, the slenderness ratio, and the steel ratio **(Rasmussen, 2000; Uy, 2000; Mursi and Uy, 2004; Ellobody and Young, 2005; Ellobody and Young, 2006; Young and Ellobody, 2006; Liu, 2006; Uy, 2008; Lam and Gardne, 2008)**. Also, the effects of the stiffeners on the CFST column stiffness and ductility were studied, such as the placement, arrangement, diameter, and number of stiffeners inside or outside the member **(Tao et al., 2000; Dabaon et al., 2009)**. Design aspects and details of stainless steel concrete-filled columns have also been considered in several studies **(Lam and Gardner, 2008; Liew et al., 2016; Wang et al., 2016)**. The contribution of material strength to the structural performance of CFST columns was also considered in several studies **(Zhang et al., 2016; Ellobody and Young, 2005; Ellobody et al., 2006)**. However, there are limited studies focused on the behavior of the CFSST column stiffened with inner carbon structural steel inside the concrete. This shortage of experimental works for studying the CFSST columns is due to the high cost of the stainless steel tube compared to the traditional steel. Finite element (FE) analysis allows studying a wide range of parameters at a low cost, and to get solid results in no time. The main objective of this study is to investigate the contribution of concrete compressive strength to the response and structural behavior of concrete-filled steel Tubular Columns through a validated FE model.

2. FINITE ELEMENT MODELING AND VALIDATION

Integral and partial differential equations are effectively solved using the Finite Element Method (FEM), making it the most widely adopted numerical technique for addressing complex problems in engineering and applied sciences. In this study, the FEM-based software ABAQUS/CAE (Version 6.14.1/2019) was employed to conduct a comprehensive analysis for the Concrete-Filled Stainless-Steel Tube (CFSST) column that is identical to an experimentally tested specimen (CFSSTCC-II-1) in a study predicted by **(Tokgoz et al.,**

2021). **Fig. 2** and **Table 1** summarize the details of the considered specimen. The finite element model consisted of three primary components: the concrete core, the encased steel section, and the surrounding steel tube, as illustrated in **Fig. 2**. All parts were modeled by C3D8R elements—eight-node linear brick elements with reduced integration—to ensure an accurate yet computationally efficient simulation. The model included 2626 elements and 4967 nodes.

The size of elements was approximately (25 mm), which achieves the mesh sensitivity. To simulate the nonlinear behavior of the concrete, the Concrete Damage Plasticity (CDP) model was adopted. This model enables a realistic representation of concrete behavior under both tensile and compressive loading conditions, as described by Coronado and Lopez **(Carlos and Maria, 2006)**. The key parameters used to explain the CDP model are summarized in **Table 2,** and the compression stress-strain relationships for the considered compressive are shown in **Fig. 3**.

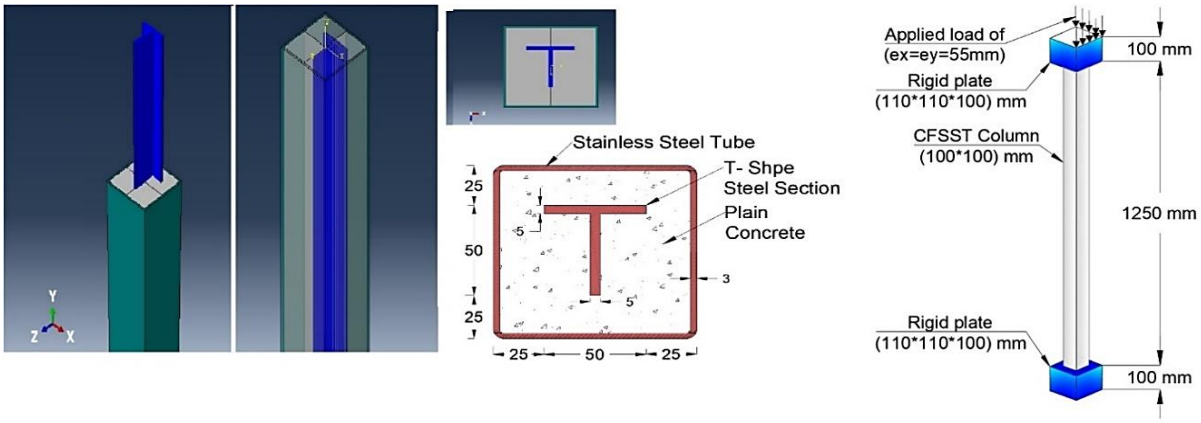

Figure 2. Details and parts of the FE model.

Table 1. Properties of the specimen CFSSTCC-II-1

f_{y-tube} (MPa)	f_{u-tube} (MPa)	$f_{y-T\,sec}$ (MPa)	$f_{u-T\,sec}$ (MPa)	E_s (GPa)	f'_c (MPa)	E_c (MPa)	e_x & e_y (mm)
550	800	290	310	200	55.6	35000	55

Table 2. Concrete damage plasticity characteristics

Variable	ψ	ε_{fp}	f_{b0}/f_{c0}	K_c	μ
Magnitude	30	0.1	1.16	0.6667	0.0001

Interactions between different model parts were carefully identified: a surface-to-surface contact interaction was used to capture the interface behavior between the concrete and the steel tube, while the encased steel section was modeled as an embedded region within the concrete core. Hinge-roller boundary conditions were applied to realistically represent the support constraints, as shown in **Fig. 4**. A displacement-controlled static explicit analysis was performed to enhance solution stability. To avoid convergence difficulties, a reduced time increment equivalent to 10% of the loading period was employed. Additionally, a constant maximum time increment was imposed, limited to 0.1 periods, to ensure numerical precision and stability throughout the simulation. The nonlinear geometry option (NLGEOM=YES) was activated in the FEM analysis to capture large deformations and geometric nonlinearity. This allowed to account for the post-buckling response of the

structure. Moreover, the equilibrium path beyond the initial buckling load was considered, thus providing a more realistic representation of the structure's behavior after buckling. The (75% damage percentage) was considered as a failure criteria control in the validation stage, but when the study extended to include the effect of the fill-concrete compressive strength, the failure criteria were changed to ensure that the parts of the CFSST Columns are mostly failed. The selected failure criteria for evaluating the outcomes (For the evaluation of failure in the concrete structures, the Concrete Damage Plasticity (CDP) model was adopted as the failure criterion. This model is widely used for simulating the nonlinear behavior of concrete under different loading conditions, as it accounts for both tensile cracking and compressive crushing.

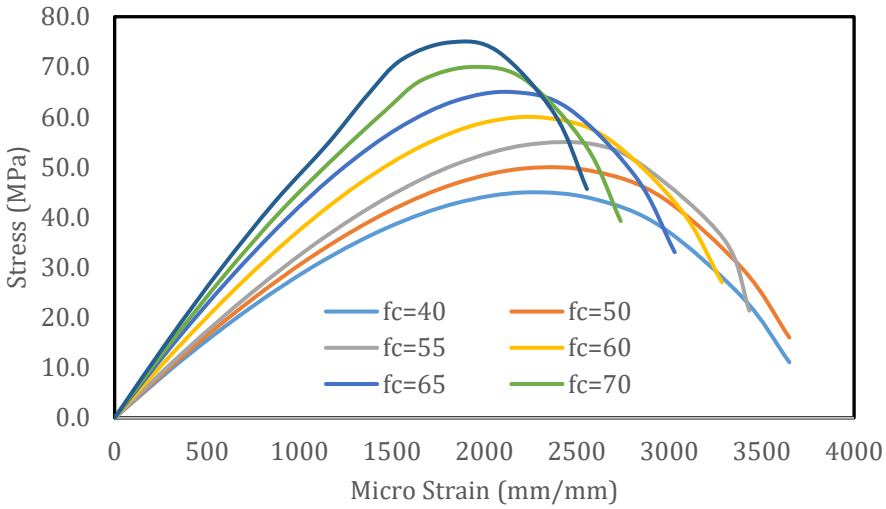

Figure 3. Compression and tension behavior of fill-concrete.

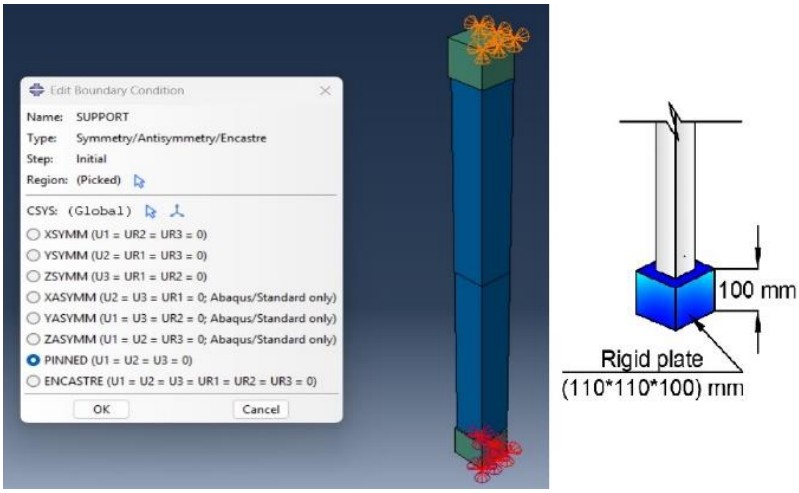

Figure 4. Details of the support in the FE model.

The CDP approach was therefore considered appropriate to capture the damage evolution and ultimate failure of the material in the present study). The accuracy of the established finite element (FE) model was assessed through a comprehensive comparison with the experimental results reported by **(Tokgoz et al., 2021)**. In particular, the model demonstrated a good association with the experimental load–deflection response in the elastic range, achieving a high level of agreement, quantified at (0.5%), as illustrated in **Fig.**

5. In the nonlinear and ultimate loading stages, the model maintained an acceptable degree of accuracy, with maximum deflection errors recorded to 1.4% and 2.6%, respectively. These values confirm the robustness and reliability of the numerical approach in capturing both linear and nonlinear structural behavior. The validation process also included a qualitative comparison of the damage patterns. The simulated damage distribution and failure mechanisms showed strong consistency with the experimentally observed patterns, further supporting the validity of the FE model, as shown in **Fig. 6**.

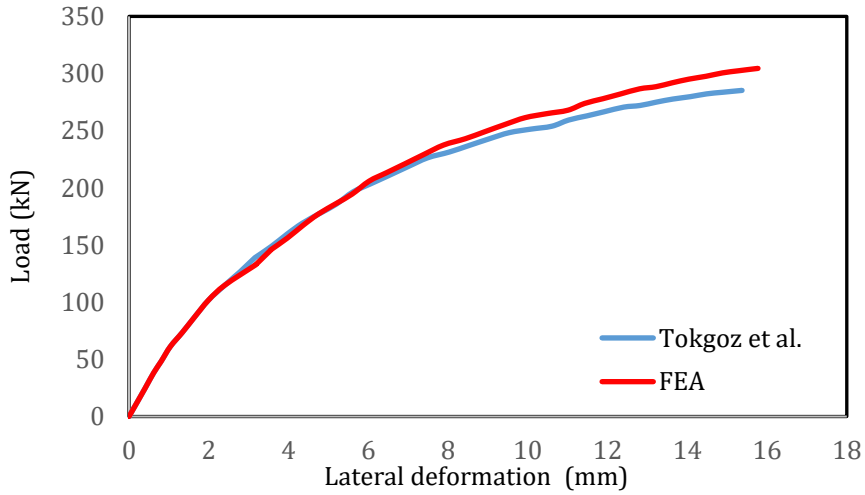

Figure 5. Validation of the FEM corresponding to the load-deflection relation.

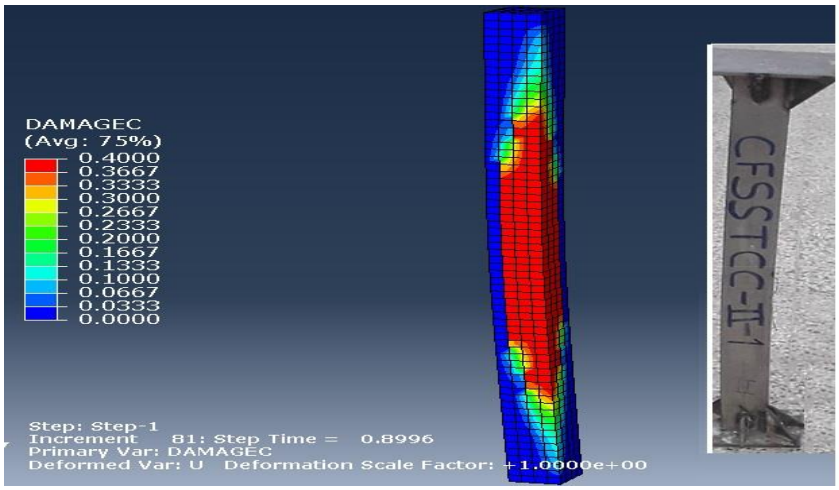

Figure 6. Validation of the FE model corresponding to the failure mode.

3. RESULTS AND DISCUSSION

The key objective of this numerical analysis is to detect the impact of concrete compressive strength on the response and structural performance of Concrete-Filled Stainless Steel Tubular Columns (CFSST). To achieve this goal, several outcomes were considered, including: load-deflection relation, ultimate and yielding load, ultimate deflection, stiffness, toughness, ductility index, and load-strain behavior for concrete and steel T-section parts.
Table 3 symmetrized the contribution of increasing concrete compressive strength on the ultimate load, yield load, and lateral deflection of the CFSST columns. Generally, increasing

the compressive strength of the fill-concrete to more than 45 MPa significantly enhanced the strength of the CFSST columns. The modification percentage for the ultimate load and yield load was (64.2 and 64.0), respectively, as the fill-concrete compressive strength increased to 75 MPa. Moreover, the corresponding deflection at the ultimate load of the case ($f_c' = 45\ MPa$) highly reflected the influence of increasing fill-concrete compressive strength on the performance of CFSST columns; the optimum enhancement percentage reached 86.8 %. Regarding the ultimate deflection at the failure stage, a reduction state was noticed as the compressive strength of the fill-concrete increased to reach (17.2%) in the case of ($f_c' = 75\ MPa$), which reflects a reduction in the ductility index.

The load-deflection behavior of the CFSST columns for all the considered filled-concrete compressive strengths (45, 50, 55, 60, 65, 70, and 75MPa) is shown in **Fig. 7**. All the analyzed columns behave in three stages, i.e., initial elastic, nonlinear hardening, and descending stages. In the first stage (approximately the first 5 mm deflection), all the curves exhibit linear behavior where the deflection is directly proportional to the load, but each has a different proportionality ratio. This ratio increased as the fill-concrete compressive strength increased, which refers to the modification of column stiffness. In the second stage, the curves became flatter, i.e., the columns' stiffness is reduced slightly till reaching the ultimate carrying load. A gradual descent in the load-deflection curves was noticed in the third stage for all the considered concrete strengths. Fill-concrete crushing, material softening, and column buckling were all behind the observed response.

Table 3. Effect of concrete compressive strength on the ultimate response.

f_c' MPa	Ultimate load		Yield load		Ultimate deflection		Corresponding deflection @ ultimate load of $f_c' = 45\ MPa$	Variation %
	P_u kN	Variation %	P_u kN	Variation %	Δ_u mm	Variation %		
45	253	---	250	---	32.6	---	24.6	---
50	285	12.7	275	10.0	32.5	0.3	12.2	62.6
55	312	23.0	310	24.0	31.2	4.3	9.4	71.2
60	344	35.9	335	34.0	30.5	6.4	7.1	78.2
65	360	42.1	360	44.0	29.2	10.4	6.1	81.3
70	401	58.2	400	60.0	27.8	14.7	4.7	85.6
75	416	64.2	410	64.0	27.0	17.2	4.3	86.8

Initial stiffness is a crucial structural parameter that controls the structural element response at the elastic stage. It is equivalent to the slope of the load-deflection curve at the elastic stage. **Table 4** illustrates the stiffness of the analyzed CFSST columns. It was detected that the fill-concrete compressive strength significantly enhanced the stiffness of the column since it directly affected the concrete elastic modulus. The optimum modification was (89.0%) in the case of ($f_c' = 75\ MPa$). The effect of the fill-concrete compressive strength extended to include the absorbed energy, as shown in **Table 4**. The absorbed energy usually defines the total area under the load-deflection or stress-strain curve. It is an indication of the overall strength of any structural element during the elastic, nonlinear hardening, and descending stages. The outcomes enormously proved the influence of increasing the fill-concrete compressive strength upon the total absorbed energy of CFSST columns. The modification percentage compared to ($f_c' = 45\ MPa$) was (12.6, 18.3, 27.4, 29.0, 36.8, and 38.9%) for the considered concrete strength (50, 55, 60, 65, 70, and 75 MPa), respectively.

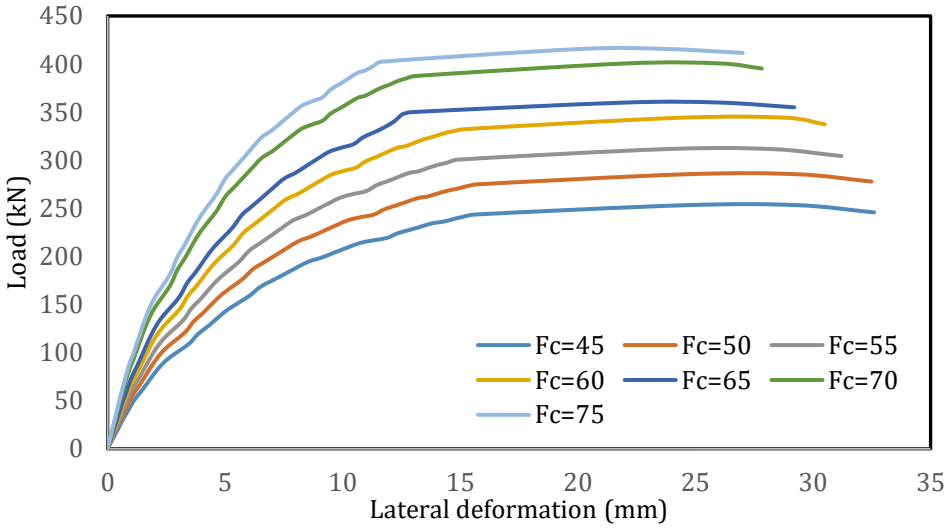

Figure 7. Effect of concrete compressive strength on the CFSST response.

One of the most important parameters to be considered in the structural safe design is the ductility index. This index characterized the ability of a structural element to undergo beyond the yielding stage, which is a very important point to avoid a brittle-sudden failure. The analysis results regarding these parameters were presented in **Table 4**. Two methods were adopted to evaluate the ductility index. The first was the energy approach developed by **(Naaman and Jeong, 1995),** as shown in **Fig. 8**. In this approach, the ductility index depends on both total and elastic energy, as illustrated in Eq. (1). It is well known that the total area under the load-deflection curve is a representative of the total energy. Regarding the elastic energy, this method performed an assumption to estimate the slope (S) of the elastic region boundary, **Fig. 8**. Dealing with a composite structural element was the reason behind adopting this method. It depends on the overall load-deflection relation rather than the yield strain of the steel part of the structural element, i.e., avoiding the selection of either the external tube or the embedded Tee-section to specify the yielding state. In the second method, displacement approach, the recognized definition of the ductility index (percentage between the ultimate and yield deflection) was considered as shown in Eq. (2). The results of the energy method reflect a negative effect on the ductility index caused by increasing the fill-concrete compressive strength where it is reduced from (3.25) to (2.75) as the fill-concrete compressive strength increased from 45 MPa to 75 MPa. High-strength concrete (HSC) is dense and less porous than normal-strength concrete (NSC). Moreover, the generated cracks in the NSC are graduate-generated cracks, while they are classified as sudden cracks in the HSC. In addition, the ultimate strain and deformability of the NSC (0.003-0.0035) are greater than those of the HSC (0.002 -0.0025), as shown in **Fig. 3**. All these reduce the ductile behavior of the CFSST columns. Even though the ductility index values of the second considered method (displacement method) were less than those of the first method (energy method), increasing the fill-concrete compressive strength still had a negative impact on the ductility index of the CFSST columns. It can be detected that a reduction from (2.55) to (1.80) was observed as the fill-concrete compressive strength increased from 45 MPa to 75 MPa.

The variation percentage between the two considered methods ranged between 22% and 35%, as illustrated in **Table 5**. Estimating the elastic level contributes to the variation between the two methods. In the displacement method, the yield deflection usually refers to

the level of steel reinforcement yielding, while the elastic energy characterizes the absorbed energy for the linear elastic behavior of the hole structure. It can also be detected that the variation is directly proportional to the fill-concrete strength.

$$\mu_{EN} = 0.5\left(\frac{E_t}{E_e} + 1\right) \quad (1)$$

$$\mu_{\Delta} = \frac{\Delta_u}{\Delta_y} \quad (2)$$

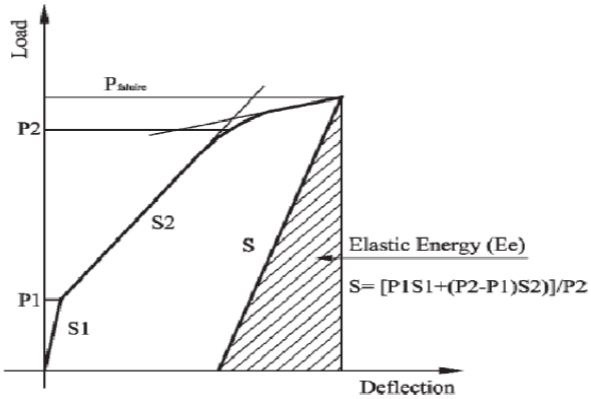

Figure 8. Details of Ductility index evaluation by energy approach **(Naaman and Jeong, 1995)**

Strain-load progress in a composite structural element is an important point that reflects the contribution of each part in the overall strength of the composite element. **Fig. 9** displays the load-strain behavior of the analyzed CFSST columns, especially the fill-concrete part at the mid-height of the column.

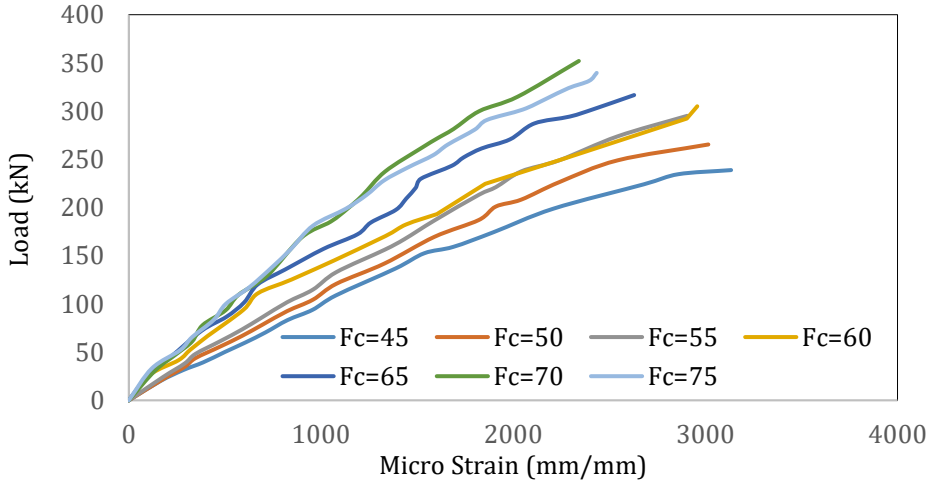

Figure 9. Effect of concrete compressive strength on the fill concrete strain.

This figure improved the effect of fill-concrete compressive strength upon the ultimate response of CFSST columns. The curves exhibited high stiffness and low ultimate strain as the compressive strength increased, which is compatible with the gained outcomes regarding the initial stiffness and ductility index of the CFSST columns. Moreover, the load corresponding to the ultimate concrete strain is less than that of the CFSST columns, i.e., the column can withstand beyond the stage of fill-concrete failure. The percentage difference between the fill-concrete and CFSST columns' failure load reduced as the compressive

strength increased to be (44.3%) for ($f'_c = 75$ MPa). The strain in the steel T-section is also considered, as shown in **Fig. 10.** The influence of the fill-concrete compressive strength significantly enhanced the yield point, i.e., extended the elastic range.

Table 4. Effect of concrete compressive strength on Stiffness and absorbed energy.

f'_c MPa	Stiffness (kN/m)	% Variation relative to $f'_c = 45\ MPa$	Toughness (kN.mm)	% Variation relative to $f'_c = 45\ MPa$
45	36229.0	---	6833	---
50	42208.5	16.5	7694	12.6
55	47822.2	32.0	8081	18.3
60	54343.4	50.0	8707	27.4
65	59491.8	64.2	8815	29.0
70	63920.6	76.4	9351	36.8
75	68489.2	89.0	9494	38.9

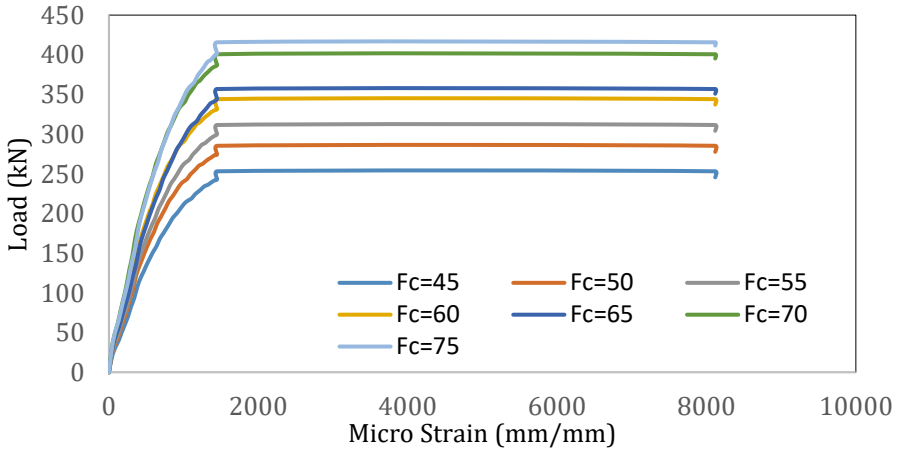

Figure 10. Effect of concrete compressive strength on the steel T-section strain.

Table 5. Ductility index of the CFSST columns.

f'_c MPa	Energy - Ductility Index (Naaman and Jeong, 1995)				$\mu_\Delta = \frac{\Delta_u}{\Delta_y}$ Based on T-sec	% Variation between the two ductility methods
	E_t	E_e	μ_{EN}	% Variation relative to $f'_c = 45$ MPa		
45	6833	1242	3.25	---	2.55	22
50	7694	1597	2.91	10.5	2.24	23
55	8081	1689	2.89	11.1	2.10	27
60	8707	1921	2.77	14.8	2.08	25
65	8815	1958	2.75	15.4	1.95	29
70	9351	2080	2.75	15.4	1.85	33
75	9494	2110	2.75	15.4	1.80	35

1. CONCLUSIONS

Depending on a validated FEM, the contribution of fill-concrete compressive strength in CFSST columns to modify the structural response was investigated. A wide range of concrete strengths was considered, including (45, 50, 55, 60, 65, 70, and 75MPa). Different parameters were adopted to attain the main objective of this study, these are: load-deflection relation, ultimate and yielding load, ultimate deflection, stiffness, toughness, ductility index, and load-strain behavior. The outcomes prove the crucial contribution of fill-concrete compressive strength. Increasing the compressive strength to (75 MPa) modifies the

structural behavior of CFSST columns, including: ultimate load, yield load, stiffness, and toughness by (64.2, 64.0, 89.0, 38.9), respectively, corresponding to (45 MPa). Another improvement was detected, but it was the opposite of the first one. Increasing the fill-concrete compressive strength from (45 MPa) to (65 MPa) reduced the ductility index of the CFSST columns by (15.4%). The percentage reduction in the ductility index up to (f'_c = 65 MPa) remains constant even though the fill-concrete compressive strength increased. Moreover, the two considered methods (energy and displacement) to evaluate the ductility index were compatible regarding the overall influence of increasing the fill-concrete compressive strength, but there was a variation percentage between the two methods outcomes ranged between (22-35)%.

NOMENCLATURE

Symbol	Description	Symbol	Description
E_t	Total energy, kN.mm.	μ	Concrete viscosity
E_e	Elastic energy, kN · mm.	ε_{fp}	Potential eccentricity flow
K_c	Ratio of the second stress invariant on the tensile meridian to that on the compressive meridian	f_{b0}/f_{c0}	Initial biaxial compressive yield stress to initial uniaxial compressive yield stress
ψ	Angle of dilation	μ_{EN}	Enerjy ductility index
& $\Delta_y \Delta_u$	Ultimate deflection and yield deflection, mm	μ_Δ	Ductility index

Credit Authorship Contribution Statement

Shatha D. Mohammed: Writing – original draft, Writing – review & editing, Validation, Methodology. Mohammed Riyadh Khalaf: Software, Writing – original draft. Teghreed H. Ibrahim: Writing – review & editing. Abbas A. Allawi: Writing – review & editing.

Declaration of Competing Interest

The authors declare that they have no known competing financial interests or personal relationships that could have appeared to influence the work reported in this paper.

REFERENCES

Alrebeh, S.K., and Ekmekyapar, T., 2019. Structural behavior of concrete-filled steel tube short columns stiffened by external and internal continuous spirals. *Structures*, 22, pp. 98–108, https://doi:10.1016/j.istruc.2019.07.001

Al-Sherrawi, M.H., Salman, H.M., and Mohammed, S.D., 2025. Analytical and theoretical development of load-moment interaction diagrams of rectangular CFRP-RC columns. *Engineering Technology Application Science Res*earch, 15(4), pp. 25178–25191, https://doi.org/10.48084/etasr.12059

Carlos, A., Coronado, and Maria, M. Lopez, 2006. Sensitivity analysis of reinforced concrete beams strengthened with FRP laminates, *Cement and Concrete Composites*, 28(1), pp. 102-114. https://doi.org/10.1016/j.cemconcomp.2005.07.005

Dabaon, M.A., El-Boghdadi, M.H., and Hassanein, M.F., 2009. Experimental investigation on concrete-filled stainless steel stiffened tubular stub columns. *Engineering Structures*, 31(2), pp. 300–307. https://doi.org/10.1016/j.engstruct.2008.08.017

Dai, X., and Lam, D., 2010. Axial compressive behaviour of stub concrete-filled columns with elliptical stainless steel hollow sections. *Steel and Composite Structures*, 10(6), pp. 517–539, https://doi.org/10.12989/scs.2010.10.6.517

Dong, H., Li, Y., Cao, W., Qiao, Q., and Li, R., 2018. Uniaxial compression performance of rectangular CFST columns with different internal construction characteristics. *Engineering Structures*, 176(1), pp. 763–775, https://doi:10.1016/j.engstruct.2018.09.05

Ellobody, E., and Young, B., 2005. Structural performance of cold-formed high strength stainless steel columns. *Journal of Constructional Steel Research*, 61(12), pp. 1631-1649. https://doi.org/10.1016/j.jcsr.2005.05.001

Ellobody, E., and Young, B., 2006. Design and behaviour of concrete-filled cold-formed stainless steel tube columns. *Engineering Structures*, 28(5), pp. 716–728. https://doi.org/10.1016/j.engstruct.2005.09.023

Ellobody, E., Young, B., and Lam, D., 2006. Behaviour of normal and high strength concrete-filled compact steel tube circular stub columns. *journal of Constructional Steel Research*, 62(7), pp. 706–715. https://doi.org/10.1016/j.jcsr.2005.11.002

Hassanein, M.F., Shao, Y.B., Elchalakani, M., and El Hadidy, A.M., 2020. Flexural buckling of circular concrete-filled stainless steel tubular columns. *Marine Structures*, 71(5), P. 102722. https://doi.org/10.1016/j.marstruc.2020.102722

Kazemzadeh Azad, S., Li, D., and Uy, B., 2021. Compact and slender box concrete-filled stainless steel tubes under compression, bending, and combined loading. *Journal of Constructional Steel Research*, 184(9), P. 106813. https://doi.org/10.1016/j.jcsr.2021.106813

Lam, D., and Gardner, L., 2008. Structural design of stainless steel concrete filled columns. *Journal of Constructional Steel Research*, 64(11), pp. 1275–1282. https://doi.org/10.1016/j.jcsr.2008.04.012

Lam, D., and Williams, C.A., 2004. Experimental study on concrete filled square hollow sections. *Steel and Composite Structures,* 4(2), pp. 95–112, https://doi.org/10.12989/scs.2004.4.2.095

Lee, S.H., Uy, B., Kim, S.H., Choi, Y.H., and Choi, S.M., 2011. Behavior of high-strength circular concrete-filled steel tubular (CFST) column under eccentric loading. *Journal of Constructional Steel Research*, 67(1), pp. 1–13. https://doi.org/10.1016/j.jcsr.2010.07.003

Liew, J.Y.R.., Xiong, M., and Xiong, D., 2016. Design of concrete filled tubular beam-columns with high strength steel and concrete. *Structures*, 8(12), pp. 213–226. https://doi.org/10.1016/j.istruc.2016.05.005

Liu, D., 2004. Behaviour of high strength rectangular concrete-filled steel hollow section columns under eccentric loading. *Thin-Walled Structures*, 42(12), pp. 1631–1644. https://doi.org/10.1016/j.tws.2004.06.002

Liu, D., 2005. Tests on high-strength rectangular concrete-filled steel hollow section stub columns. *Journal of Constructional Steel Research*, 61(7), pp. 902–911. https://doi.org/10.1016/j.jcsr.2005.01.001

Liu, D., 2006. Behaviour of eccentrically loaded high-strength rectangular concrete-filled steel tubular columns. *Journal of Constructional Steel Research*, 62(8), pp. 839–846. https://doi.org/10.1016/j.jcsr.2005.11.020

Manikanta, K., Hanumantha Rao, C., and Siva Kishore, I., 2020. Investigation on structural behavior of concrete filled stainless steel tubular stub columns. *Materials Today: Proceedings*, 33(1), pp. 964–972. https://doi.org/10.1016/j.matpr.2020.06.525

Mursi, M., and Uy, B., 2004. Strength of slender concrete filled high strength steel box columns. *Journal of Constructional Steel Research*, 60(12), pp. 1825–1848. https://doi.org/10.1016/j.jcsr.2004.05.002

Naaman, A.E., and Jeong, S.M., 1995. Structural ductility of concrete beams prestressed with FRP tendons, non-metallic (FRP) reinforcement for concrete structures. *Proceedings of the Second International RILEM Symposium, L. Taerwe, ed., CRC Press, Boca Raton, FL,* pp. 379-386.

Rasmussen, K.J.R., 2000. Recent research on stainless steel tubular structures. *Journal of Constructional Steel Research*, 54(1), pp. 75–88. https://doi.org/10.1016/S0143-974X(99)00052-8

Salman, H.M., and Al-Sherrawi, M.H. 2024. M-N Interaction diagrams of RC columns strengthened with steel C-sections and battens. *Civil Engineering Journal*. 10(6), pp. 1974–1986, https://doi.org/10.28991/CEJ-2024-010-06-016

Tao, Z., Ha,n L.H., and Wang, D.Y., 2007. Experimental behaviour of concrete-filled stiffened thin-walled steel tubular columns. *Thin-Walled Structures*, 45(5), pp. 517–527. https://doi.org/10.1016/j.tws.2007.04.003

Tokgoz, S., Dundar, C., Karaahmetli, S., and Ozel, R., 2021. Research on concrete-filled stainless steel tubular composite columns. *Structures*, 33, pp. 703–719, https://doi.org/10.1016/j.istruc.2021.04.065

Uy, B., Tao, Z., and Han, L.H., 2011. Behaviour of short and slender concrete-filled stainless steel tubular columns. *Journal of Constructional Steel Research*, 67(3), pp. 360–378, https://doi.org/10.1016/j.jcsr.2010.10.004

Uy, B., 2000. Strength of concrete-filled steel box columns incorporating local buckling. , *Journal of Structural Engineering. ASCE*, 126(3), pp. 341–352. https://doi.org/10.1061/(ASCE)0733-9445(2000)126:3(341)

Uy, B., 2008. Stability and ductility of high performance steel sections with concrete infill. *Journal of Constructional Steel Research*, 64(7-8), pp. 748–754. https://doi.org/10.1016/j.jcsr.2008.01.036

Wang, X., Liu J., and Zhou, X., 2016. Behaviour and design method of short square tubed-steel-reinforced-concrete columns under eccentric loading. *Journal of Constructional Steel Research*, 116(1), pp. 193–203. https://doi.org/10.1016/j.jcsr.2015.09.018

Young, B., and Ellobody, E., 2006. Experimental investigation of concrete-filled cold-formed high strength stainless steel tube columns. *Journal of Constructional Steel Research*, 62(5), pp. 484–492. https://doi.org/10.1016/j.jcsr.2005.08.004

Zeghiche, J., and Chaoui, K., 2005. An experimental behaviour of concrete-filled steel tubular columns, *Journal of Constructional Steel Research*, 61(1), pp. 53–66, https://doi.org/10.1016/j.jcsr.2004.06.006

Zhang, T., Ding, F., Wang, L., Liu, X., and Jiang, G., 2018. Behavior of polygonal concrete-filled steel tubular stub columns under axial loading. *Steel Composite Structures*, 28(5), pp. 573–588. https://doi.org/10.12989/scs.2018.28.5.573

مساهمة مقاومة انضغاط الخرسانة الحشوية في الأداء الإنشائي لأعمدة(CFSST) : دراسة تحليلية

شذى ضياء محمد*، محمد رياض خلف، تغريد حسن ابراهيم، عباس عبد المجيد ذياب

قسم الهندسة المدنية، كلية الهندسة، جامعة بغداد، بغداد، العراق

الخلاصة

تُعد المنشات الشاهقة الارتفاع مؤشرًا مهمًا في التطور الحضري المعاصر، وخاصة في المناطق التي تتميز بالنمو الحضري المتسارع والكثافة السكانية. يصمم هذا النوع من المباني لتحمل ظروف الأحمال الشديدة. لذلك، فإن استخدام العناصر الهيكلية المركبة في مثل هذه الهياكل مطلوب لتوفير مزيد من القوة والديمومة. تقدم هذه الورقة نموذج تحليلي باعتماد طريقة العناصر المحدودة المحددة للأعمدة الأنبوبية المصنوعة من الفولاذ المقاوم للصدأ والمملوءة بالخرسانة (CFSST) ذات المقطع العرضي (100 × 100) مم وطول (1250) مم لفحص تأثير قوة انضغاط الخرسانة على استجابة اعمدة (CFSST) . في البدء, تم تقييم النموذج التحليلي من خلال مقارنة شاملة مع بحث تجريبي، وبعد ذلك تم استخدام النموذج لدراسة المعاملات المعتمدة، أي قوة انضغاط الخرسانة. تم تضمين مجموعة واسعة من قوى ضغط الخرسانة (45 و50 و55 و60 و65 و70 و75) ميجا باسكال. أشارت نتائج العناصر المحدودة إلى أن القوة القصوى لأعمدة CFSST تتناسب طرديًا مع قوة انضغاط الخرسانة الحشوية. بلغت أقصى قدرة تحميل مكتسبة (416 كيلو نيوتن) عند قوة تحمل الخرسانة 75 ميجا باسكال. وامتد تحسين زيادة قوة ضغط الخرسانة الحشوية ليشمل الصلابة والمتانة وحمل الخضوع ليصبح (89، 38.9، و64%) على التوالي، مع زيادة قوة الانضاط إلى 75 ميجا باسكال. ولم يشمل تحسن الاستجابة مؤشر اللدونة. ولوحظ انخفاض في مؤشر اللدونة مع زيادة قوة انضغاط الخرسانة الحشوية ليصل إلى 15.4% عند 65 ميجا باسكال. يستمر هذا الانخفاض ثابتًا حتى مع زيادة قوة الضغط الى (70 و75 ميجا باسكال).

الكلمات المفتاحية: اعمدة (CFSST)، قوة انضغاط الخرسانة، معامل اللدونة، الصلابة، الطاقة الممتصة.